University of Wollongong

Research Online

1-1-2013

Effects of membrane fouling on N-nitrosamine rejection by nanofiltration and reverse osmosis membranes

Takahiro Fujioka
University of Wollongong, tf385@uowmail.edu.au

Stuart J. Khan
University Of New South Wales, s.khan@unsw.edu.au

James A. McDonald
University Of New South Wales

Rita K. Henderson
University Of New South Wales, r.henderson@unsw.edu.au

Yvan Poussade
Veolia Water Australia, yvan.poussade@veoliawater.com.au

See next page for additional authors

Follow this and additional works at: https://ro.uow.edu.au/engpapers

Part of the Engineering Commons

https://ro.uow.edu.au/engpapers/5190

Recommended Citation

Authors

Takahiro Fujioka, Stuart J. Khan, James A. McDonald, Rita K. Henderson, Yvan Poussade, Jorg E. Drewes, and Long Nghiem

Effects of membrane fouling on N-nitrosamine rejection by nanofiltration and reverse osmosis membranes

Revised version submitted to

Journal of Membrane Science

September 2012

Takahiro Fujioka [1], Stuart J. Khan [2], James A. McDonald [2], Rita K. Henderson [2], Yvan Poussade [3,4], Jörg E. Drewes [2, 5], and Long D. Nghiem [1,*]

[1] Strategic Water Infrastructure Laboratory, School of Civil Mining and Environmental Engineering, The University of Wollongong, NSW 2522, Australia

[2] UNSW Water Research Centre, School of Civil and Environmental Engineering, The University of New South Wales, NSW 2052, Australia

[3] Veolia Water Australia, Level 15, 127 Creek Street, QLD 4000, Australia

[4] Seqwater, Level 2, 240 Margaret St, Brisbane City QLD 4000 Australia

[5] Advanced Water Technology Center (AQWATEC), Department of Civil and Environmental Engineering, Colorado School of Mines, Golden, CO 80401, USA

_____

* Corresponding author: Long Duc Nghiem, Email: longn@uow.edu.au, Ph +61 2 4221 4590

LIST OF FIGURES

Figure 1: Molecular structure and molecular weight of the selected N-nitrosamines.

Figure 2: Fouling development procedure and N-nitrosamine rejection measurement.

Figure 3: LC-OCD chromatograms of tertiary effluent, SA, BSA and HA solutions. OCD and UVD represent organic carbon detection and UV-detection at 254 nm, respectively.

Figure 4: Normalised permeate flux of the ESPAB, ESPA2 and NF90 membranes as a function of filtration time using the tertiary effluent (crossflow velocity 40.2 cm/s, feed temperature 20.0 ± 0.1 ℃).

Figure 5: Normalised permeate flux of the ESPA2 membrane as a function of filtration time using (a) SA, (b) HA, (c) BSA and (d) Ludox CL (20 mM NaCl, 1 mM $NaHCO_3$, 1 mM $CaCl_2$, cross flow velocity 40.2 cm/s, feed pH 8.0 ± 0.1, feed temperature 20.0 ± 0.1 ℃). Open and solid symbol indicates the result of the first and second experiment, respectively.

Figure 6: Effects of membrane fouling by tertiary effluent (TE) and model foulants (SA, BSA, HA and Ludox CL) on contact angle of the NF90, ESPA2 and ESPAB membranes. Error bars show the standard deviation of two replicate experiments.

Figure 7: Effects of membrane fouling by tertiary effluent (TE) and model foulants (BSA, HA and Ludox CL) on zeta potential of the ESPA2 membrane. The measurement was conducted in 1mM KCl at $25\pm1°C$.

Figure 8: Conductivity rejection of the clean and fouled membranes (Permeate flux 20 L/m^2h, crossflow velocity 40.2 cm/s, feed temperature 20.0 ± 0.1 ℃). Error bars show the standard deviation of two replicate experiments.

Figure 9: Effects of membrane fouling using tertiary effluent on the rejection of N-nitrosamines by (a) ESPAB, (b) ESPA2 and (c) NF90 membranes (permeate flux 20 L/m^2h, cross flow velocity 40.2 cm/s, feed temperature 20.0 ± 0.1 ℃). Error bars on the ESPA2 membranes show the standard deviation of two replicate experiments. N-nitrosamine concentrations (except NDMA and NMOR) in the permeate of the ESPAB membrane were all below detection limits.

Figure 10: N-nitrosamine rejections by the ESPA2 membrane with and without fouling of (a) SA, (b) HA, (c) BSA and (d) Ludox CL. (20 mM NaCl, 1 mM NaHCO$_3$, 1 mM CaCl$_2$, permeate flux 20 L/m^{2}h, cross flow velocity 40.2 cm/s, feed pH 8.0 ± 0.1, feed temperature 20.0 ± 0.1 ℃). Error bars show the standard deviation of two replicate experiments.
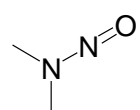
NDMA
(74 g/mol)
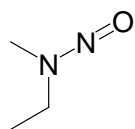
NMEA
(88 g/mol)
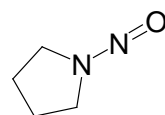
NPYR
(100 g/mol)

NDEA
(102 g/mol)

NPIP
(114 g/mol)

NMOR
(116 g/mol)

NDPA
(130 g/mol)

NDBA
(158 g/mol)

Figure 1

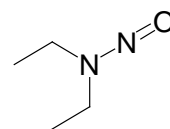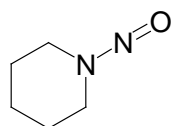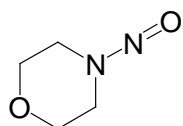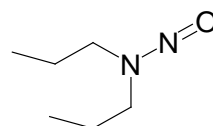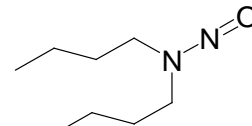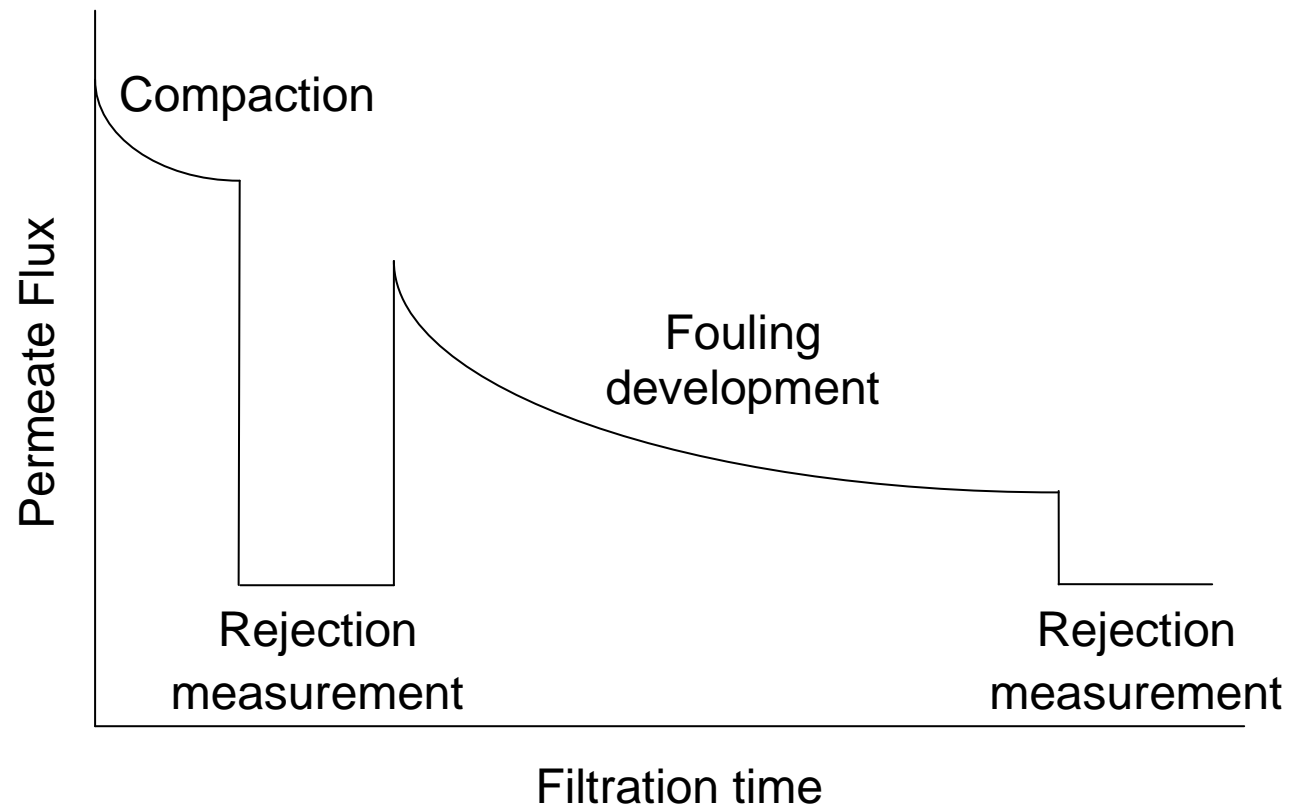**Figure 2**
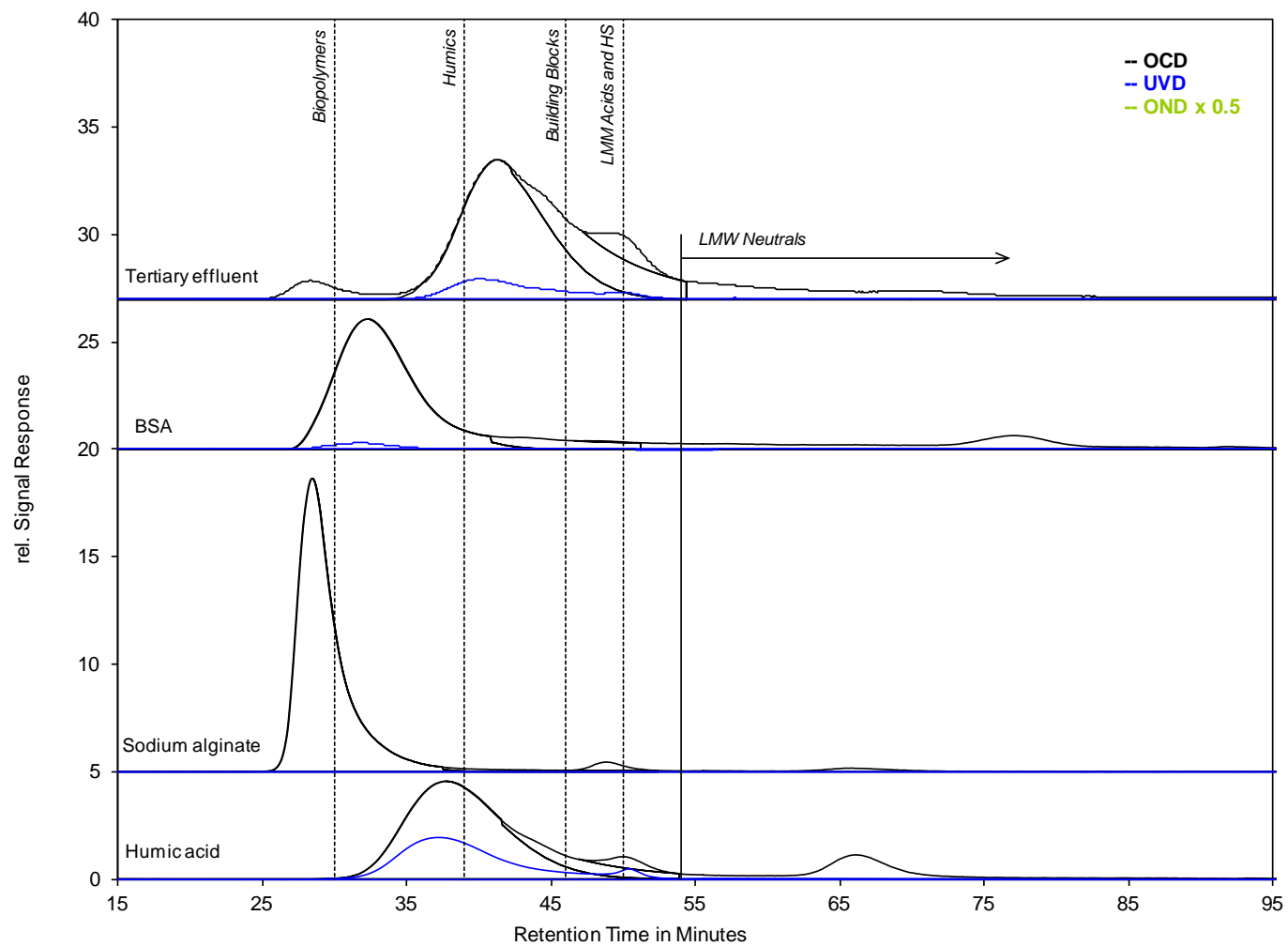
Figure 3
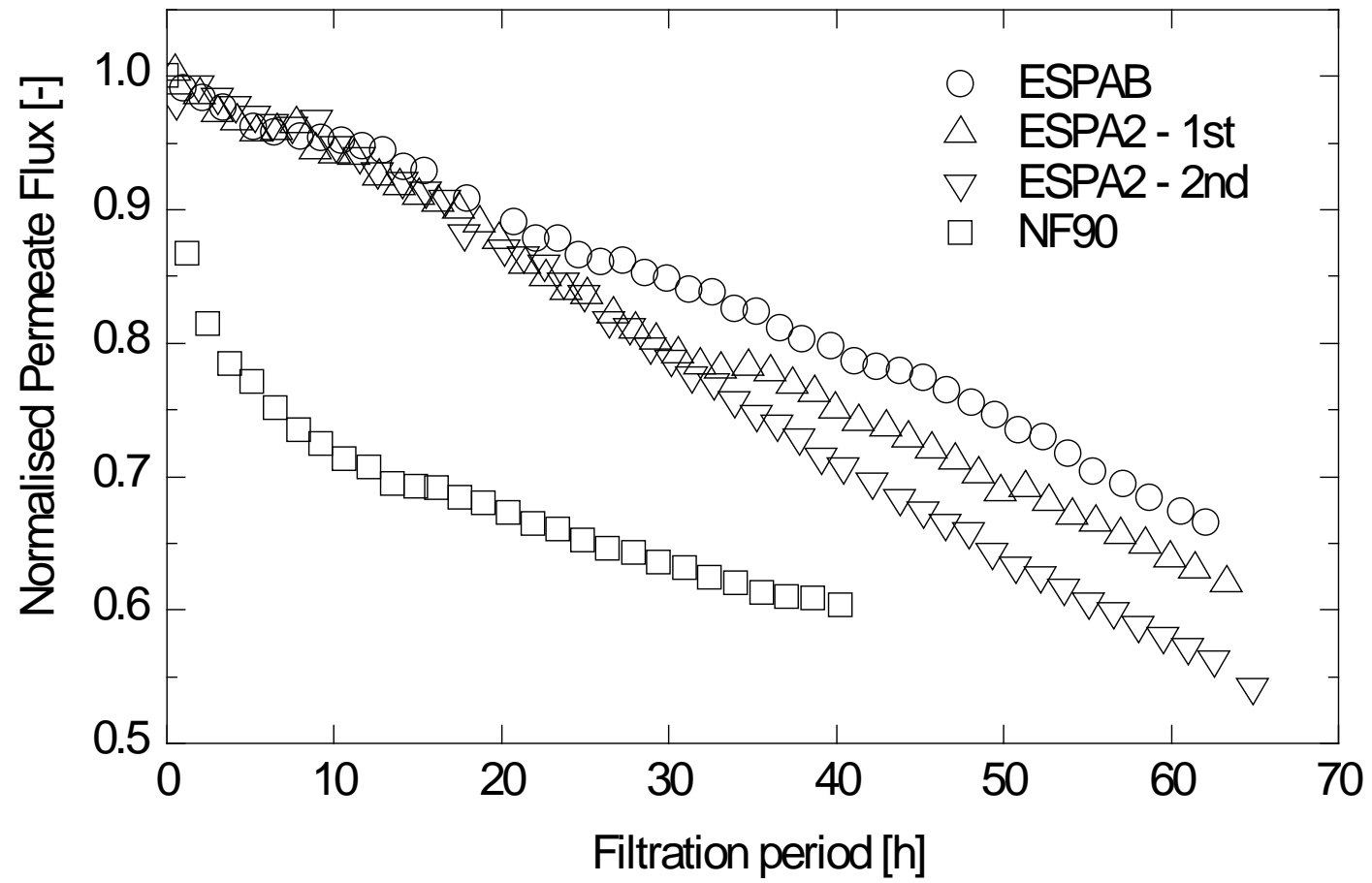
Figure 4
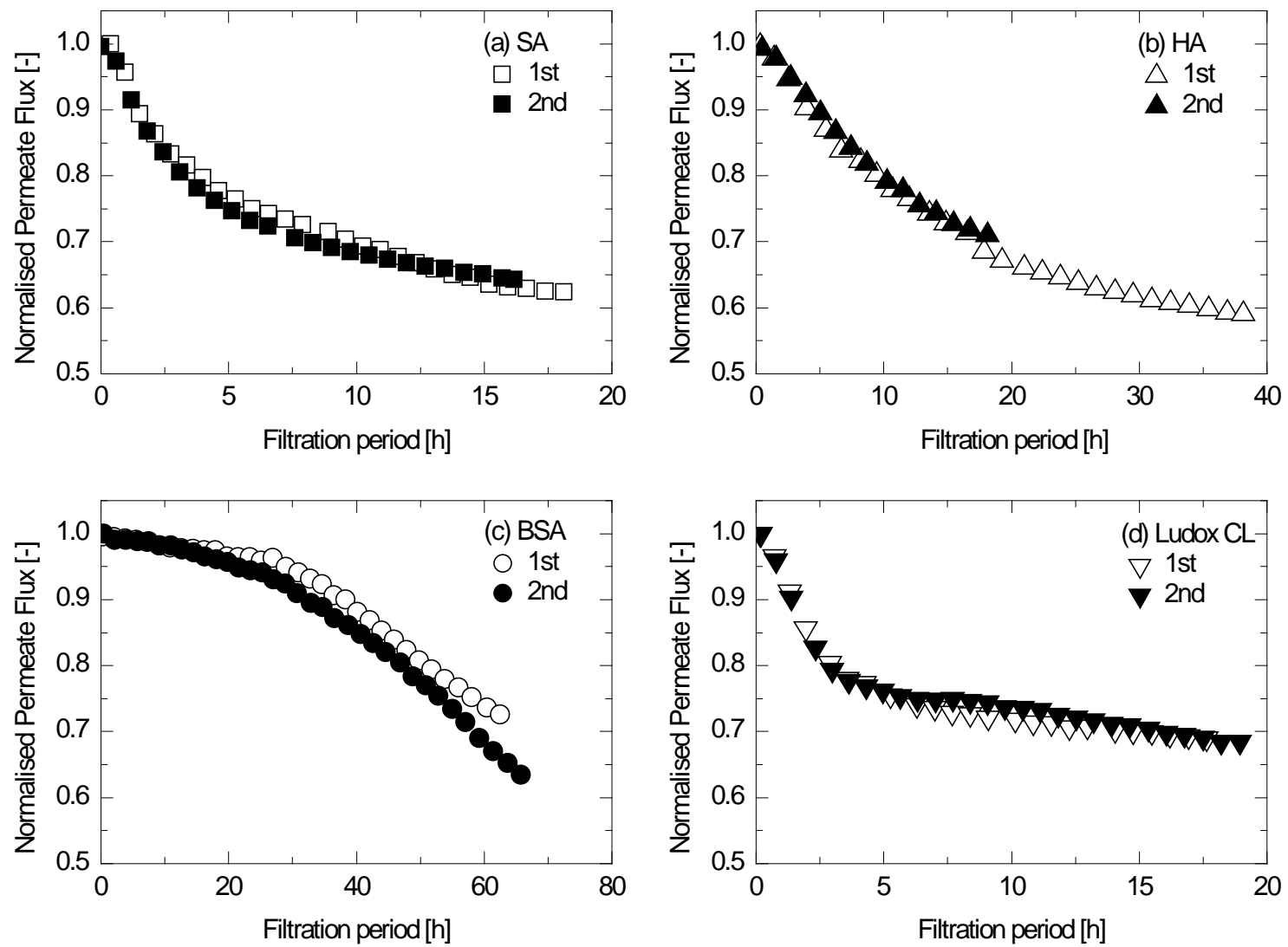
Figure 5
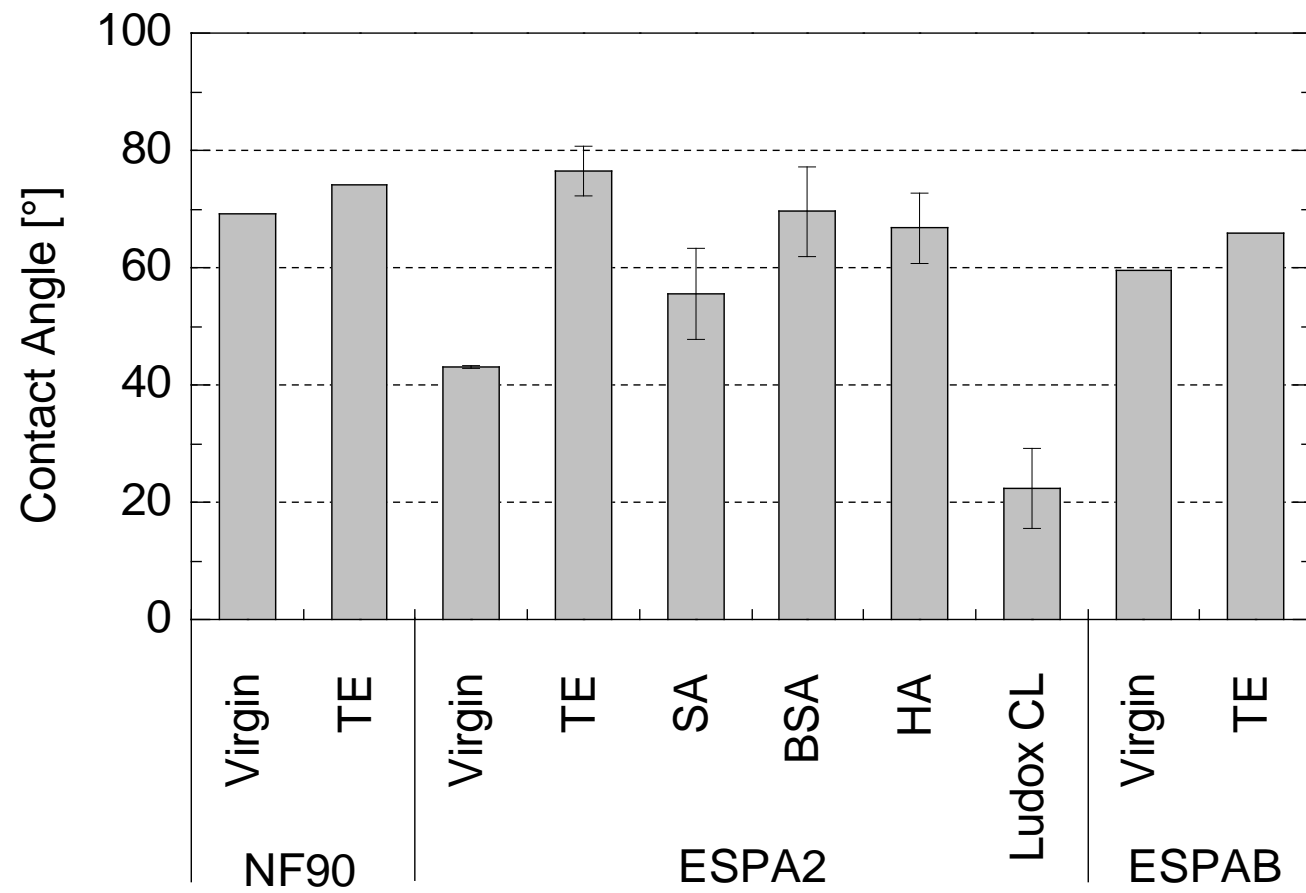
Figure 6
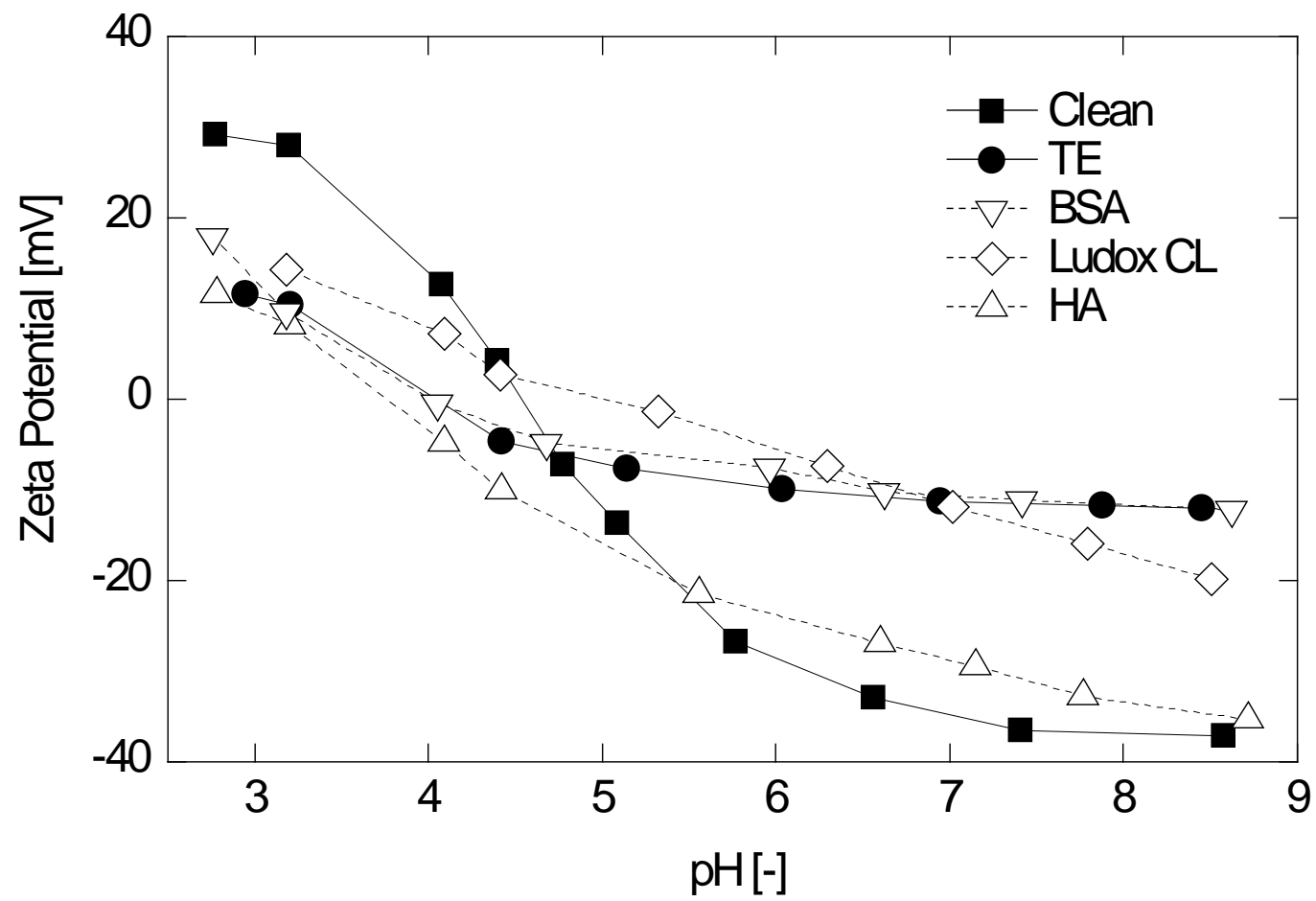
Figure 7
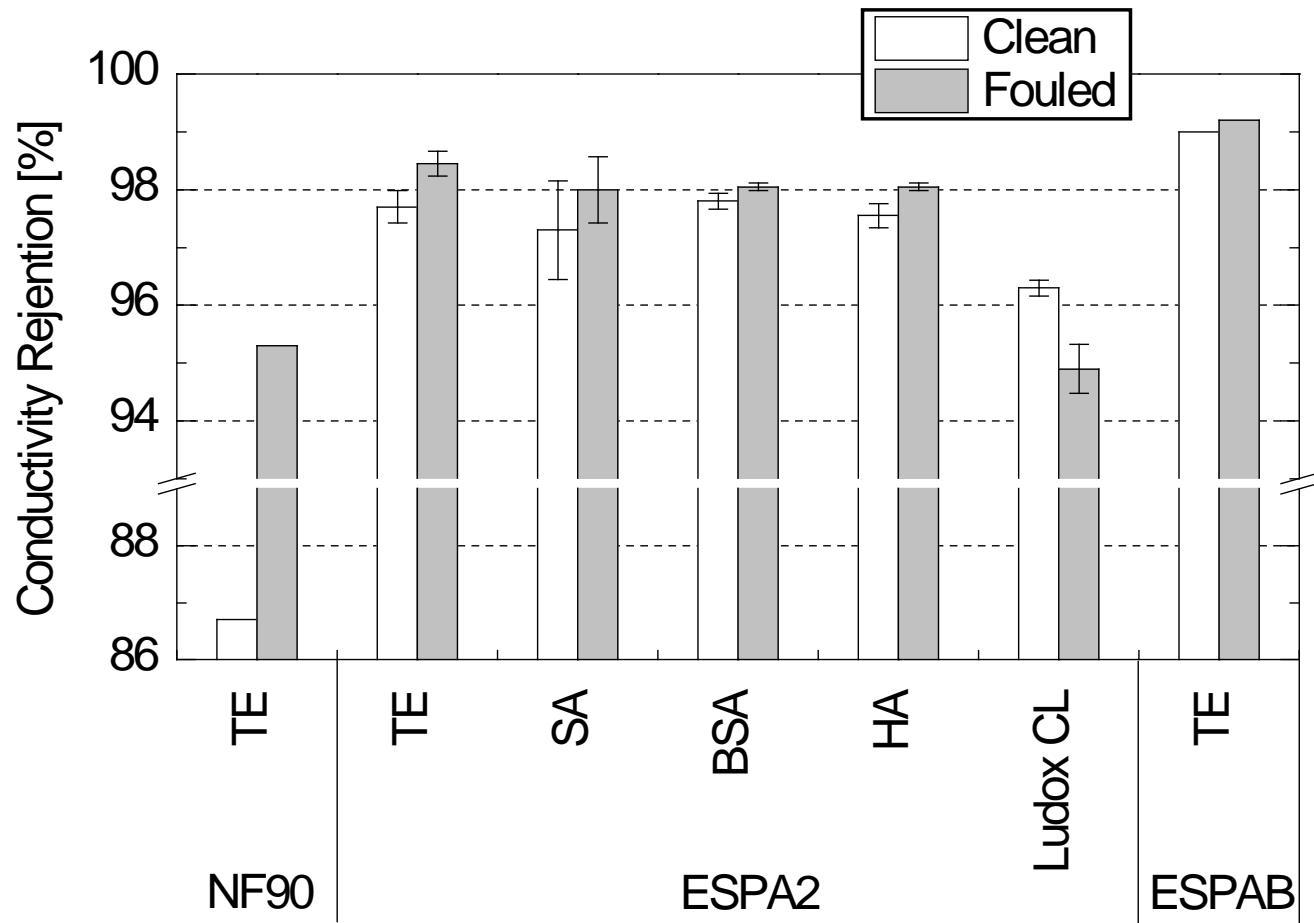
Figure 8

1031

1032 **Figure 9**

32
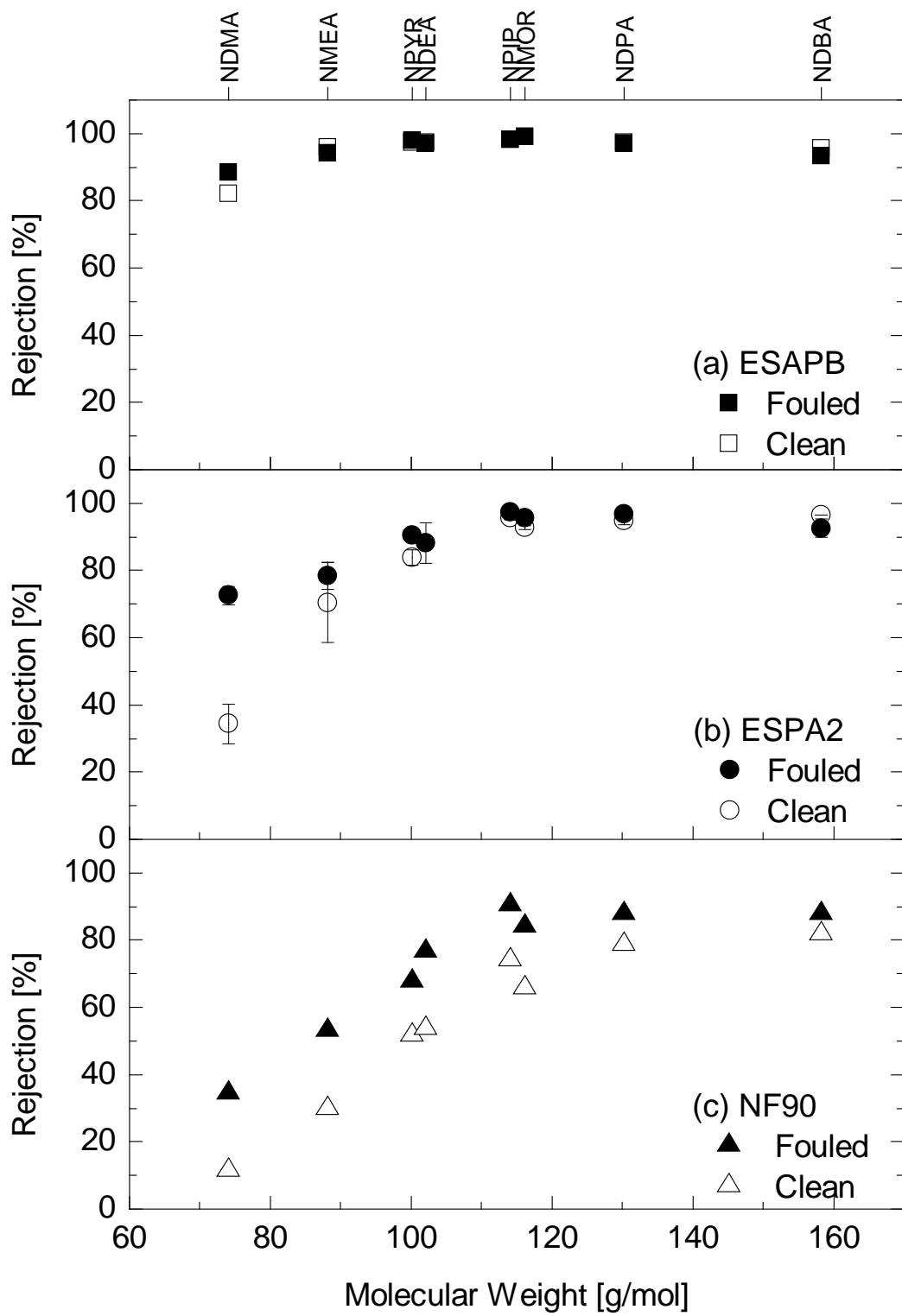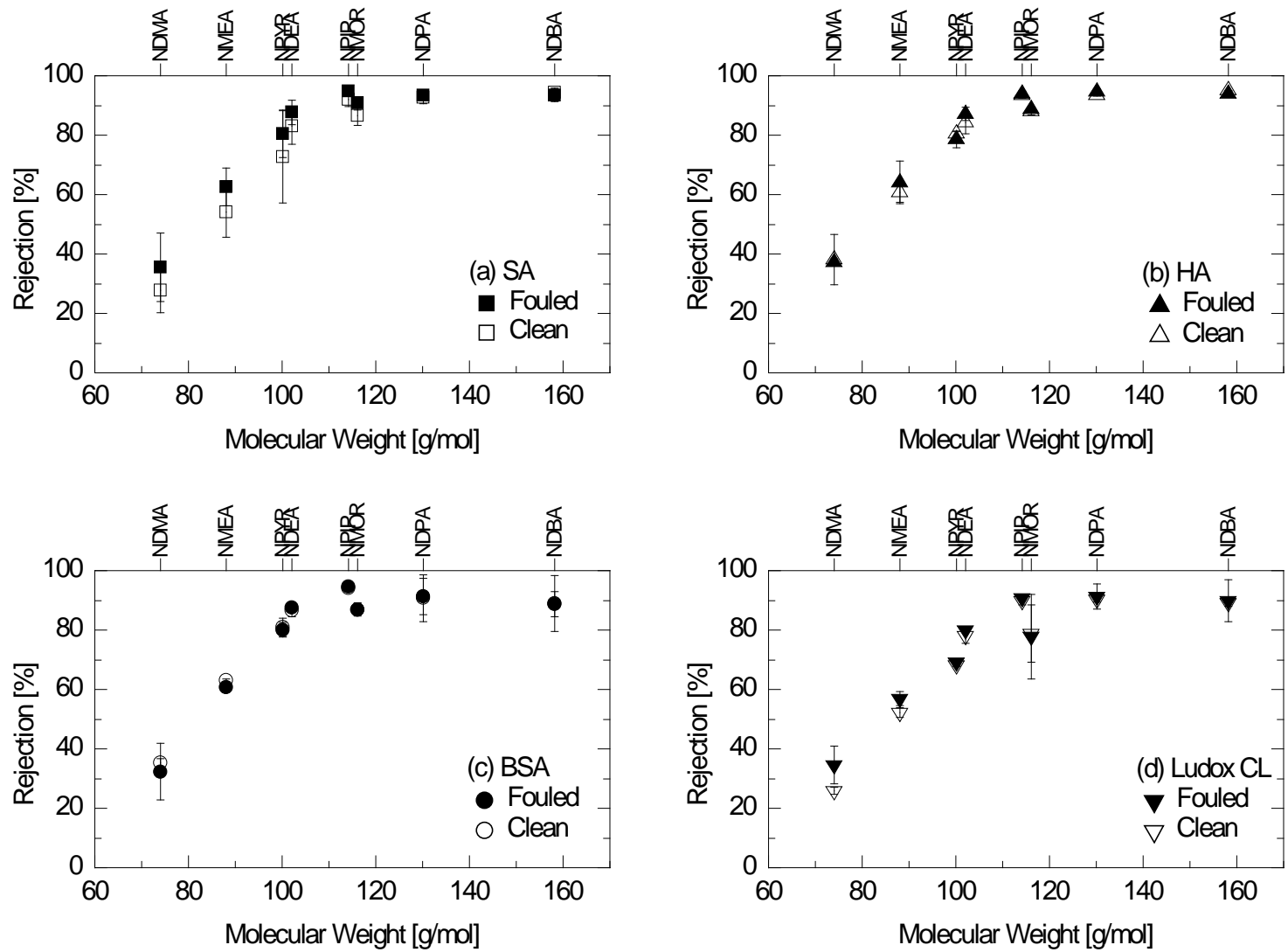
Figure 10

1 Abstract

2 The impact of fouling on N-nitrosamine rejection by nanofiltration (NF) and reverse osmosis

3 (RO) membranes was investigated in this study. Membrane fouling was simulated using

4 tertiary treated effluent and several model fouling solutions (that contained sodium alginate,

5 bovine serum albumin, humic acid or colloidal silica) to elucidate the changes in rejection

6 behaviour of N-nitrosamines. In general, the rejection of N-nitrosamines increased when the

7 membranes were fouled by tertiary effluent. The rejection of small molecular weight N-

8 nitrosamines was most affected by membrane fouling. In particular, the rejection of N-

9 nitrosodimethylamine (NDMA) by the ESPA2 membrane increased from 34 to 73% after

10 membrane fouling caused by tertiary effluent. The results also indicate that the impact was

11 less apparent for the lowest permeability membrane (i.e., ESPAB), and the rejection of N-

12 nitrosamines by the ESPAB membrane was over 82% regardless of membrane fouling. The

13 effect of membrane fouling caused by model foulants on N-nitrosamine rejection was

14 considerably less than that caused by tertiary effluent. Size exclusion chromatography

15 analyses revealed that the tertiary effluent contains a high fraction of low molecular weight (<

16 500 g/mol) organic substances. It appears that these low molecular weight foulants present in

17 the tertiary effluent can restrict the solute pathway within the active skin layer of membranes,

18 resulting in the observed increase of solute rejection.

19 **Keywords:** Water recycling, N-nitrosamines, NDMA, reverse osmosis, organic fouling,

20 colloidal fouling.

21

1. Introduction

Augmentation of potable water sources with reclaimed municipal effluent is an important strategy to secure a reliable water supply in regions and countries with severe water scarcity. However, a major concern over this alternative source of water supply is the occurrence of trace organic chemicals which may induce adverse and chronic health effects. Notable amongst these trace organic chemicals is N-nitrosodimethylamine (NDMA) which is an N-nitrosamine that can be formed during the chloramination of the treated effluent [1]. In addition to NDMA, other N-nitrosamines known to occur in treated effluent include N-nitrosomethylethylamine (NMEA), N-nitrosopyrrolidine (NPYR), N-nitrosodiethylamine (NDEA), N-nitrosopiperidine (NPIP), N-nitrosomorpholine (NMOR), N-nitrosodipropylamine (NDPA), N-nitrosodi-n-butylamine (NDBA) [2-4]. Some of these N-nitrosamines have been identified as probable carcinogenic agents and thus their concentrations in drinking water and recycled water intended for potable consumption have been regulated by water authorities around the world [5-6]. The Australian Guidelines for Water Recycling have recommended the maximum value of NDMA, NDEA, and NMOR in recycled water intended for potable supply of 10, 10, and 1 ng/L, respectively [7]. Both reverse osmosis (RO) and nanofiltration (NF) membranes have been frequently used in water reclamation partly to ensure adequate removal of emerging trace chemicals, little is known about their capacity to remove N-nitrosamines in full-scale installations. Reported percentage rejections of NDMA vary greatly in full-scale plants from almost negligible to 86% and the underlying reason for such significant variation in NDMA rejection remains unclear [8-11].

To date, only a few laboratory-scale studies have investigated N-nitrosamine rejection capability of NF/RO membranes using clean matrix solutions [3, 12-13]. These studies reported that the rejection of NDMA by RO membranes was in the range from 50 to 70%. The rejection of N-nitrosamines increased in the order of increasing molecular weight and the steric hindrance mechanism was identified as a predominant rejection mechanism of N-nitrosamines by NF/RO membranes [3, 12-13]. Feed solution characteristics (i.e., pH, ionic strength and temperature of the feed solution) also affected the rejection of NDMA and in some cases other N-nitrosamines [3, 13]. In particular, Fujioka et al. [13] reported a significant drop in NDMA rejection (from 49 to 25%) for an increase in feed temperature from 20 to 30 ℃. Nevertheless, the variations in these feed solution characteristics explain

53　only some of the variations in NDMA rejections that were reported in the previous full-scale
54　studies.

55　Municipal wastewater usually contains a large amount of organic and inorganic matter,
56　resulting in the formation of organic and colloidal fouling, bio-fouling and inorganic scales
57　on RO membranes [14-15]. It has been established in the literature that membrane fouling
58　can either increase or decrease the separation efficiency of NF/RO membranes [14, 16-18].
59　However, apart from a laboratory-scale study conducted by Steinle-Darling et al. [3] who
60　investigated the rejection of several N-nitrosamines by an RO membrane (ESPA3) artificially
61　fouled with sodium alginate, to date little attention has been given to the effects of membrane
62　fouling on the rejection of N-nitrosamines. Steinle-Darling et al. [3] reported that membrane
63　fouling by sodium alginate on the ESPA3 membrane caused a reduction in NDMA rejection
64　(from 56 to 37%).

65　The aim of this work was to provide insights into the effects of membrane fouling on the
66　rejection of N-nitrosamines by NF/RO membranes. The effects of membrane fouling were
67　investigated by comparing the rejections of N-nitrosamines by clean and fouled membranes.
68　Tertiary treated effluent and four different model foulants (namely sodium alginate, bovine
69　serum albumin, humic acid and colloidal silica) were used to induce membrane fouling. The
70　tertiary treated effluent and model foulants were characterised in detail to systematically
71　elucidate the effects of membrane fouling on the rejection of N-nitrosamines by NF/RO
72　membranes.

2.　Materials and methods

2.1. NF/RO membranes

75　Three NF/RO membranes – namely the NF90, ESPA2, and ESPAB – were used in this
76　investigation. These are thin-film composite polyamide membranes with a microporous
77　supporting layer and were supplied as flat sheet samples. Key properties of these membranes
78　are shown in Table 1. The NF90 (Dow Filmtec, Minneapolis, MN, USA) is an NF membrane
79　typically used for softening of brackish water. The ESPA2 (Hydranautics, Oceanside, CA,
80　USA) is a low pressure reverse osmosis membrane that is widely applied for water
81　reclamation applications. The ESPAB (Hydranautics, Oceanside, CA, USA) is also low
82　pressure reverse osmosis but it has been designed to achieve a high boron rejection.

3

83   **[Table 1**]

2.2. Chemicals

The eight N-nitrosamines used in this study (Figure 1) were of analytical grade and were purchased from Sigma-Aldrich (St Louis, MO, USA). Their physicochemical properties have been described in detail elsewhere [13]. N-nitrosamine stock solution was prepared in pure methanol with 250 µg/L of each N-nitrosamine. A deuterated surrogate standard was used for each N-nitrosamine under investigation. These surrogate standards include N-nitrosodimethylamine-D6, N-nitrosomethylethylamine-D3, N-nitrosopyrrolidine-D8, N-nitrosodiethylamine-D10, N-nitrosopiperidine-D10, N-nitrosomorpholine-D8, N-nitrosodipropylamine-D14 and N-nitrosodi-n-butylamine-D9, and were purchased from CDN isotopes (Pointe-Claire, Quebec, Canada). A surrogate stock solution containing 100 µg/L of each deuterated N-nitrosamine was prepared in pure methanol. The stock solutions were stored at -18 ºC and used within one month of preparation.

Analytical grade NaCl, $CaCl_2$ and $NaHCO_3$ were purchased from Ajax Finechem (Taren Point, NSW, Australia). Sodium alginate (SA), bovine serum albumin (BSA), humic acid (HA) and colloidal silica (Ludox CL, 30% weight suspension in water) were selected as model foulants to simulate polysaccharides, proteins, refractory organic matter and colloidal particles, respectively. These model foulants were purchased from Sigma-Aldrich (St Louis, MO, USA). The Ludox CL is a positively charged silica particle whose surface is coated with a layer of aluminium [19]. The hydrodynamic diameter of the Ludox CL is from approximately 40 nm at below pH 6 to 233 nm at pH 10 due to aggregation effects in different pH solutions [19].

105   **[Figure1]**

2.3. Tertiary treated effluent

Tertiary treated effluent sample was collected from an advanced water recycling plant in New South Wales, Australia. The treatment train of the plant prior to the sampling point includes screening, bioreactor and sand filtration, and the sample was collected after sand filtration.

2.4. Membrane filtration system

A laboratory-scale cross flow NF/RO filtration system was used in this study (Supplementary Material Figure S1). A detailed description of this system is available elsewhere [13]. The system consisted of a cross-flow stainless steel cell with effective membrane area of 4 cm by 10 cm and a channel height of 2 mm. The feed solution was kept in a stainless reservoir and was fed to the membrane cell by a high pressure pump (Hydra-Cell, Wanner Engineering Inc., Minneapolis, MN, USA). The permeate flow and cross-flow velocity were regulated by a bypass valve and a back-pressure regulator (Swagelok, Solon, OH, USA). The permeate flow was monitored using a digital flow meter (FlowCal, GJC Instruments Ltd, Cheshire, UK) which was connected to a computer. A stainless steel heat exchanging coil was submerged into the feed reservoir and was connected to a chillier/heater unit (Neslab RTE 7, Thermo Scientific Inc., Waltham, MA, USA) to control the temperature of the feed solution.

2.5. Experimental protocols

Rejection measurement and membrane fouling development were sequentially carried out with four steps: (1) compaction; (2) measuring N-nitrosamine rejection without membrane fouling; (3) fouling development; and (4) remeasuring N-nitrosamine rejection by fouled membrane (Figure 2). Because full-scale RO plants are generally operated with a constant (average) permeate flux which is approximately 20 L/m^2h [20] and feed pressure increases as fouling progresses to maintain the permeate flux, the constant permeate flux of 20 L/m^2h was used to evaluate N-nitrosamine rejection before and after fouling. Throughout the experiments, cross flow velocity and feed temperature in the reservoir were always kept constant at 0.42 m/s and 20 $\pm$ 0.1 ℃, respectively. The details of these four steps are as follows.

Step 1: The membrane sample was first compacted using Milli-Q water at 1,800 kPa until the permeate flux was stabilised.

Step 2: Following the compaction step, the Milli-Q water in the filtration system was replaced with either the tertiary effluent or synthetic solution containing a particular model foulant (e.g. SA, HA, BSA or Ludox CL) and background electrolytes (20 mM NaCl, 1 mM $CaCl_2$ and 1 mM $NaHCO_3$). The concentrations of SA, BSA and HA in the feed solution were adjusted to make up approximately 10 mg/L as total organic carbon (TOC). The Ludox

140   CL was suspended in the same background electrolyte solution (20 mM NaCl, 1 mM CaCl$_2$

141   and 1 mM NaHCO$_3$) to obtain 100 mg/L of colloidal silica. After the replacement of feed

142   solutions, stock N-nitrosamine solution was spiked into the feed solution at environmentally

143   relevant concentration (i.e., 250 ng/L). The permeate flux was also adjusted at 20 L/m^{2}h

144   which is a typical value for most water reclamation RO plants [20]. The system was operated

145   for 1 h prior to the collection of the feed and permeate samples for analysis. This sampling

146   point represents the performance of the membrane under a clean condition.

147   Step 3: After the first sampling event, membrane fouling was promoted by adjusting the

148   permeate flux to 60 L/m^{2}h. The system was then continuously operated with a constant feed

149   pressure. The fouling development step ended after the permeate flux reached 45 L/m^{2}h (i.e.,

150   decreased by 25%).

151   Step 4: The permeate flux was adjusted to 20 L/m^{2}h and the system was stabilised for 1 h

152   prior to the second sampling of the feed and permeate. This sampling point represents the

153   performance of the membrane under a fouled condition.

154   **[Figure 2]**

2.6. Analytical techniques

2.6.1.   Size exclusion chromatography analyses

157   Characterisation of dissolved organic carbon (DOC) composition in the tertiary effluent and

158   model foulant solution samples was carried out with a size exclusion chromatography

159   technique using a Liquid Chromatography - Organic Carbon Detection (LC-OCD) Model 8

160   system (DOC-LABOR, Karlsruhe, Germany). The LC-OCD system is equipped with a UV-

161   detector (254 nm) as well as organic carbon and nitrogen detectors. Chromatographic

162   separation is undertaken using a Toyopearl$^®$ TSK HW-50S column (Tosoh Bioscience,

163   Tokyo, Japan). Prior to the analysis, calibration of humic substance molecular weights was

164   conducted using IHSS Humic acid and IHSS Fulvic acid. Calibrations of detectors for total

165   organic carbon and total organic nitrogen were also conducted using potassium hydrogen

166   phthalate and potassium nitrate, respectively. For the analysis, a mobile phase (phosphate

167   buffer, pH 6.37, 2.5 g/L KH$_2$PO$_4$ and 1.5g/L Na$_2$HPO$_4$·H$_2$O) was set at a flow rate of   1.1

168   mL/min. In the LC-OCD system, an injected sample of 1 mL was pre-filtered with an in-line

169   0.45 µm PES-filter located in front of the column and detectors. Software provided by the
170   manufacturer (ChromCALC, DOC-LABOR, Karlsruhe, Germany) was used for the
171   quantification of the organic matter compositions. Further details can also be found in
172   previous studies [21-22].

173   2.6.2. Contact angle measurement

174   Contact angle of membrane surface was measured using the standard sessile drop method.
175   This was performed with a Rame-Hart Goniometer (Model 250, Rame-Hart, Netcong, NJ).
176   Prior to the measurement, virgin and fouled membrane samples were dried for over 24 h in
177   the dark. The dry membrane was fixed on the stage of the instrument and contact angle of the
178   membrane was measured with a water droplet (Milli-Q water). The contact angle of each
179   membrane was determined with an average of ten droplets.

180   2.6.3. Zeta potential measurement

181   Zeta potential of the virgin and fouled membrane surface was determined and calculated
182   using the Fairbrother-Mastin streaming potential method. The measurement of the streaming
183   potential was performed between pH 3 and 8.5 with a SurPASS Electrokinetic Analyser
184   (Anton Paar GmbH, Graz, Austria).   In the measurement, 1 mM KCl was used as a
185   background electrolyte solution. The background solution pH was adjusted by a titration of
186   either KOH (1M) or HCl (1M) solutions. During the analysis, the background solution
187   temperature was $25\pm1°C$.

188   2.6.4. Basic analytical techniques

189   Turbidity was analysed using a 2100N laboratory turbidity meter (Hach, USA). Conductivity
190   and pH were measured using an Orion 4-Star Plus pH/conductivity meter (Thermo scientific,
191   USA). TOC concentration was determined using a TOC-VSH analyser (Shimadzu, Japan)
192   based on the non-purgeable organic carbon (NPOC) method. Cations and anions were
193   analysed using an Inductive Coupled Plasma – Mass Spectrometer (7500CS, Agilent
194   Technologies, Wilmington, DE, USA) and an ion chromatography (IC) system (Shimadzu,
195   Tokyo, Japan), respectively.

196   2.6.5. N-nitrosamine concentration analysis

197   The analysis of each N-nitrosamine concentration in this study is based on the gas

198   chromatography coupled with tandem mass spectrometry (GC-MS/MS) technique using

199   electron ionisation in a combination with the solid phase extraction (SPE) method previously

200   described by McDonald et al [23]. Prior to the SPE process, the SPE cartridges

201   (Supelclean[TM] Coconut Charcoal SPE cartridges (2 g/mL), Supelco, St Louis, MO, USA)

202   were cleaned with 6 mL dichloromethane, 6 mL methanol and 12 mL of Milli-Q water.

203   Accurate quantitation (accounting for incomplete SPE recovery) was undertaken by direct-

204   analogue isotope dilution for all nitrosamines by adding 100 µL surrogate stock solution into

205   200 mL of each sample to make up 50 ng/L of each N-nitrosamine surrogate. N-nitrosamines

206   in the samples were then extracted by SPE at a flow rate of 5 mL/min. The cartridges were

207   rinsed with 3 mL Milli-Q water and dried with high purity nitrogen gas for at least 60

208   minutes. The dried SPE cartridges were then eluted using 12 mL dichloromethane, and 100

209   µL of toluene was added in the eluent. The eluent was then concentrated to 1 mL with a

210   Turbovap LV (Caliper Life Sciences, Hopkinton, MA, USA) under a gentle nitrogen stream.

211   The concentrations of N-nitrosamines were quantified using an Agilent 7890A gas

212   chromatograph (GC) coupled with an Agilent 7000B triple quadrupole mass spectrometer

213   (MS/MS). Calibration curves were established for each N-nitrosamine in the range of 1-400

214   ng/L. The NMOR calibration curve was extended to account for the NMOR concentration of

215   over 400 ng/L. The quantitative detection limits of this technique for NDMA, NDEA and

216   NDPA were 5 ng/L. The quantitative detection limits for all other N-nitrosamines used in this

217   study were 10 ng/L.

3. Results and discussion

218

3.1. Characteristics of the tertiary effluent and model foulants

219

220   Ionic composition and organic content of the tertiary effluent used in this study (Table 3) was

221   similar to that of most water reclamation plants. Nevertheless, the conductivity of this tertiary

222   treated effluent (Table 2) was slightly lower than the typical range of 1200-1700 µS/cm,

223   which is often found in the literature [24-25]. The tertiary effluent used in this study had not

224   been subjected to chloramination, with the exception of NMOR, and all other N-nitrosamines

225   were not detectable in the tertiary effluent sample. The concentration of NMOR in this

226   tertiary effluent was 1350 ng/L. NMOR can be found in toiletry and cosmetic products [26]

227 and rubber and tire industry, elevated concentration of NMOR in treated effluent has
228 previously been reported [27]. The water recycling plant where the tertiary treated effluent
229 was collected is known to have a very high load of industrial wastewaters in its catchment.

230 **[Table 2]**

231 The organic contents of secondary effluents have been generally characterised to comprise a
232 number of size fractions commonly referred to as biopolymers (polysaccharides, proteins and
233 colloidal organics) (>>20,000 Da), humic substances (approximately 1000 Da), building
234 blocks (300-500 Da) and low molecular weight (LMW) acids (<350 Da) and neutrals (<350
235 Da) [21-22, 28-29]. The building blocks block fraction represents breakdown products, or
236 intermediates during the degradation, of humic substances such as fulvic acid [22, 30]. The
237 tertiary effluent used in this study has a diverse molecular weight distribution (Figure 3). The
238 DOC concentration of fractions of biopolymers (10%), humic substances (46%), building
239 blocks (17%) and LMW neutrals (23%) in the tertiary effluent (Table 3) was in good
240 agreement with a previous study carried out by Henderson et al. [28]. Model foulants used in
241 this investigation had significant differences in their physicochemical characteristics which
242 were expected to assist in identifying the impact of fouling on membrane separation
243 performance. The major fraction of SA and BSA solutions was biopolymers (>20000 g/mol),
244 which is consistent with a previous study [31] showing a molecular weight of 12000-80000
245 g/mol (SA) and 67000 g/mol (BSA). The molecular weight of HA analysed here was in the
246 range of approximately 1000 g/mol and this is in good agreement of the average molecular
247 weight of HA (1000 g/mol) reported in the literature [22]. All three organic model foulant
248 also contained some fraction of building blocks (300-500 g/mol) and LMW neutrals (<350
249 g/mol) (Table 3).

250 **[Figure 3]**

251 **[Table 3]**

252 *3.2. Membrane fouling behaviour*

253 Significant membrane fouling was observed with all three membranes investigated in this
254 study when tertiary effluent was used at the elevated initial permeate flux of 60 L/m^{2}h (which
255 is approximately three times the value used in most full scale RO systems for water recycling

9

256 applications). The profile of membrane permeability measured before and after fouling is
257 presented in Table S2 of the Supplementary Material. Membrane fouling behaviour of the
258 NF90 differs significantly from that of the ESPA2 and ESPAB membranes (Figure 4). Flux
259 decline was most severe for the NF90 membrane followed by the ESPA2 and ESPAB
260 membranes. The permeate flux of the NF90 membrane dropped by 30% within the first 12 h
261 system operation, and then decreased linearly as filtration progressed. In contrast, the two RO
262 membranes (ESPAB and ESPA2) showed an almost linear flux decline from the beginning of
263 the filtration. The flux decline of the ESPA2 and ESPAB membranes using tertiary effluent
264 reached 30% with 40-50 h and 60 h filtration, respectively. Interestingly, the rate of flux
265 decline amongst the three membranes increased in the order of increasing pure water
266 membrane permeability (Table 1). Similar observations were reported in previous laboratory-
267 scale studies [16, 32].

268   **[Figure 4]**

269 When the model foulants were used, significant variation in membrane fouling was observed.
270 When the ESPA2 membrane was fouled with either SA or HA, permeate flux dropped
271 rapidly within 10–20 h of system operation (Figure 5a-b). These observed curves of
272 membrane fouling are consistent with a previous study [33]. The rapid flux decline in the
273 early stage may have resulted from the formation of an alginate and humic acid fouling layer
274 on the membrane surface, resulting in a substantial resistance to permeate flow [16, 34]. In
275 fact, it is known that the HA foulant layer can account for a cake layer as thick as 4 µm [35],
276 while a skin layer thickness of RO membrane is usually less than 0.3 µm [36]. In contrast,
277 membrane fouling by BSA used here progressed slowly and linearly until 30 h system
278 operation, and then the slope of the permeate flux decline became steeper (Figure 5c). This
279 trend of the permeate flux decline is again in good agreement with a previous study [31].
280 Permeate flux with Ludox CL dropped significantly within 5 h of system operation, then
281 gradually decreased as filtration progressed (Figure 5d). This observation is consistent with a
282 previous laboratory-study from which it was suggested that the hydrophobic interactions and
283 electrostatic attraction forces between charged colloid particles and membrane surface were
284 key causes for colloidal membrane fouling in the early filtration stage [19].

285   **[Figure 5]**

10

3.3. *Characteristics of fouled membranes*

The membrane surface hydrophobicity (measured by contact angle) increased significantly when the NF/RO membranes were fouled by tertiary effluent (Figure 6). The contact angle of the ESPA2 membrane increased from 43 to 79º due to the membrane fouling. While the three virgin membranes (NF90, ESPA2 and ESPAB) have a wide range of contact angle values (43-69º), the fouled membrane surface revealed a very similar contact angle (in the range of 66-79º). The type of foulants can also have a major impact on the hydrophobicity of membranes. The hydrophobicity of ESPA2 membranes increased as a result of membrane fouling by SA, HA and BSA, whereas a considerable reduction in hydrophobicity was observed with Ludox CL (Figure 6). The contact angle of each fouled membrane analysed here was in good agreement with results reported by Beyer et al. [33] who also investigated the hydrophobicity of fouled membranes by various model foulants using the NF270 membrane. Results reported here suggest that the hydrophobicity of the fouled membrane surface depends mainly on the hydrophobicity of the foulants.

The impact of fouling on the membrane surface charge was also examined by analysing zeta potentials of clean and fouled ESPA2 membranes. Consistent with a previous study [35], the zeta potential of the fouled membranes became less negative at high pH (i.e., pH8) and less positive at low pH (Figure 7). Amongst the model foulants, the zeta potential of BSA was similar to tertiary effluent at all pH values tested. Although organic matter eluting in tertiary effluent has a high concentration of material with similar molecular size to humic substances (Table 3), the measured zeta potential of fouled membranes by the tertiary effluent and HA were distinctly different (Figure 7). These results suggest that the material of the tertiary effluent eluting in the humic substance fraction is similar to humic acid and fulvic acid standards in terms of molecular size but has different charge characteristics. It is noted that the zeta potential analysis of the SA fouled membrane was not conducted because of the re-formation of alginate gel which clogged of the flow through cell of the Electrokinetic Analyser.

[Figure 6]

[Figure 7]

11

3.4. Effects of membrane fouling on inorganic salt retention

Membrane fouling by tertiary effluent led to an increase in conductivity (salt) rejection for all membranes with an exception of Ludox CL used in this investigation (Figure 8). In particular, conductivity rejection by the NF90 membrane increased significantly from 87 to 95%. Similarly, when the ESPA2 membrane was fouled by organic model foulants (SA, HA and BSA), conductivity rejection also increased. Because the fouling layer and skin layer surfaces of the RO membranes were negatively charged at pH 8 (Figure 7), the conductivity rejection increase may be attributed to an additional repelling force occurring between the fouling layer and salts. Tang et al. [32] investigated the impact of humic acid fouling using several NF/RO membranes and suggested that an increase in conductivity rejection with humic acid fouling may be attributed to an increase in repelling force between Cl$^-$ anions and the cake layer where negatively charged humic acid is deposited (Donnan exclusion mechanism). In addition to the additional repelling force, conductivity rejection can increase when the pathways of the solute such as membrane pore (or so-called free-volume space in polymer chain [37]) and the local defects of the active skin layer are restricted with foulants. Tu et al. [38] reported a considerable increase in boron rejection when organic fouling occurred, and they suggested that the increase in boron rejection was due to the plugging of local defects or hot spots on the membrane active skin layer. In the present work, low molecular weight organic foulants present in the tertiary effluent may have narrowed down the pores within the active skin layer and/or blocked the local defects on the active skin layer surface. This additional restriction of the solute pathway may explain why the increase in conductivity rejection observed using tertiary effluent was higher than that using BSA despite their similar zeta potential of fouled membrane surface. On the other hand, the results reported here also revealed a reduction in conductivity rejection with Ludox CL fouling. Colloidal cake fouling layer depositing on membrane surface hinders back diffusion of rejected salt from the membrane surface to bulk solution, and the higher concentration gradient across the membrane is likely to result in a decrease in salt rejection (cake enhanced concentration polarisation) [31, 39]. Because the fouled membrane by colloids remarkably decreased salt rejection from 96.3% to 94.9%, the cake enhanced concentration polarisation may have played an important role in salt rejection using the fouled membrane.

[Figure 8]

12

3.5. Effects of membrane fouling on N-nitrosamine rejection

The rejection of small organic compounds by NF/RO membranes can be governed by steric hindrance, electrostatic interactions and adsorption onto the membrane surface [40]. All N-nitrosamines used are hydrophilic and uncharged at neutral pH, thus the electrostatic interactions and adsorption effects do not play a major role on their rejection performances. Previous studies also reported that N-nitrosamine rejection by NF/RO membranes in clean water matrices reached a steady state condition within a 45 min filtration period [3, 12]. Preliminary experimental results (Supplementary Material Figure S3) revealed no significant changes in the rejection of N-nitrosamines with the exception of NDEA after 1 and 48 h of filtration even in tertiary effluent feed. These results indicate that 1 h filtration is sufficient to evaluate the rejection of most N-nitrosamines in tertiary effluent. During the preliminary experiment, the concentration of some N-nitrosamines (i.e, NDMA, NMEA and NDBA) in the feed decreased as the filtration progressed. These N-nitrosamines have been reported to be readily biodegradable [4], and the reduction in these N-nitrosamines was possibly caused by biodegradation. A previous laboratory-scale study using the TFC-HR membrane [13] and preliminary experimental results using the ESPA2 membrane (Supplementary Material Figure S4) revealed that the effect of feed N-nitrosamine concentration on their rejections by these RO membranes is negligible in the range from 0.25 to 1.5 µg/L of each N-nitrosamine. Although the impact of N-nitrosamine concentration may vary depending on the specific membrane, the changes in N-nitrosamine feed concentration observed in this study are not expected to play an important role in the evaluation of N-nitrosamine rejections.

In general, membrane fouling by tertiary effluent caused an increase in N-nitrosamine rejection (Figure 9). This was particularly apparent for low molecular weight N-nitrosamines such as NDMA. For example, the rejection of NDMA by the NF90 and ESPA2 membranes increased in the range from 11 to 34% and from 34 to 73%, respectively. In contrast, membrane fouling on the ESPAB membrane resulted in only a slight increase (from 82 to 88%) in NDMA rejection. The results reported here also indicate that the ESPAB membrane is very effective for the removal of N-nitrosamines regardless of membrane fouling. As expected, during these filtration tests the concentrations of NDMA, NMEA and NDBA in the feed (i.e., tertiary effluent) decreased by up to 82%. The impact of SA fouling was minor, but nevertheless discernible for low molecular weight N-nitrosamines such as NDMA (Figure

10). On the other hand, membrane fouling of HA, BSA and Ludox CL had a negligible impact on the rejection of N-nitrosamines.

The clear difference in the impact of membrane fouling observed between tertiary effluent (Figure 9) and model foulants (Figure 10) is intriguing. For the separation mechanism of N-nitrosamines, the rejection of N-nitrosamines by NF/RO membranes has been reported to be mainly governed by steric hindrance where the interaction between N-nitrosamine molecule size and pore size of the active skin layer plays an important role in their rejection [13]. Because the molecular size of N-nitrosamines does not change under the experimental conditions, the increased rejection of some N-nitrosamines using the tertiary effluent is likely to be attributed to changes in membrane characteristics. It can be suggested that the pathway of solutes (such as membrane pore and local defects of the active skin layer) on RO membranes can be restricted with foulants present in the tertiary effluent (Section 3.4) or due to cake layer compression caused by the applied pressure increase, and these changes in the solute pathway leads to an increase of N-nitrosamine rejection.

[Figure 9]

[Figure 10]

4. Conclusions

Membrane fouling by tertiary effluent and organic model foulants (i.e., sodium alginate, bovine serum albumin and humic acid) led to an increase in conductivity rejection due to enhanced electrostatic interactions between the fouling layer and inorganic salts. On the other hand, colloidal fouling using Ludox CL caused a reduction in conductivity retention. Membrane fouling by tertiary effluent also increased the rejection of N-nitrosamines. The rejection of low molecular weight N-nitrosamines such as NDMA was most affected by membrane fouling and the impact was most pronounced for membranes that have high membrane permeability. Although the ESPA2 and ESPAB membranes were comparable in terms of membrane permeability and fouling susceptibility the rejection of N-nitrosamines by the ESPAB membrane was very high (over 82%) regardless the impact of membrane fouling. In contrast to the results using tertiary effluent, membrane fouling by model foulants revealed only a negligible impact on N-nitrosamine rejection. Because the tertiary effluent used in this investigation contained a high fraction of low molecular weight organic substances, these

407　foulants may have restricted the pathway of solutes on the active skin layer of the RO

408　membrane, resulting in an increase in N-nitrosamine rejection. The present findings provide

409　valuable insights for predicting NDMA rejection variations observed during full-scale RO

410　plant operation. In addition, the results reported here indicate that changes in NDMA

411　rejection may be predicted by analysing conductivity rejection because both rejections

412　increased as fouling progressed. During a full-scale RO plant operation fouled membranes

413　are generally cleaned by chemical cleaning when membrane permeability drops by 15-20%.

414　Future work is, therefore, necessary to examine the impact of chemical cleaning on the

415　rejection of N-nitrosamines.

6. References

[1]　A.D. Shah, W.A. Mitch, Halonitroalkanes, Halonitriles, Haloamides, and N-Nitrosamines: A Critical Review of Nitrogenous Disinfection Byproduct Formation Pathways, Environ. Sci. Technol., 46 (2011) 119-131.

[2]　Y.-Y. Zhao, J. Boyd, S.E. Hrudey, X.-F. Li, Characterization of new Nitrosamines in drinking water using liquid chromatography tandem mass spectrometry, Environ. Sci. Technol., 40 (2006) 7636-7641.

[3]　E. Steinle-Darling, M. Zedda, M.H. Plumlee, H.F. Ridgway, M. Reinhard, Evaluating the impacts of membrane type, coating, fouling, chemical properties and water chemistry on reverse osmosis rejection of seven nitrosoalklyamines, including NDMA, Water Res., 41 (2007) 3959-3967.

[4]　J.E. Drewes, C. Hoppe, T. Jennings, Fate and transport of N-Nitrosamines under conditions simulating full-scale groundwater recharge operations, Water Environ. Res, 78 (2006) 2466-2473.

[5]　USEPA, Integrated Risk Information System (IRIS), in, U.S. Environmental Protection Agency, 1993.

15

439   [6]   IARC, IARC monographs on the evaluation of carcinogenic risks to humans: Overall
440   evaluations of carcinogenicity: An updating of IARC monographs volumes 1 - 42:
441   Supplement 7, International agency for research on cancer, (1987).

442   [7]   NRMMC, EPHC, AHMC, Australian guidelines for water recycling: Managing health
443   and environmental risks (Phase 2): Augmentation of drinking water supplies,
444   Environment Protection and Heritage Council, National Health and Medical Research
445   Council, Natural Resource Management Ministerial Council, Canberra, 2008.

446   [8]   R. Lugg, Characterising treated wastewater for drinking purposes following reverse
447   osmosis treatment, Premier's Collaborative Research Program, (2009).

448   [9]   D. Sedlak, M. Kavanaugh, Removal and destruction of NDMA and NDMA
449   precursors during wastewater treatment, in, WateReuse Foundation, Alexandria, VA,
450   2006.

451   [10]   M.H. Plumlee, M. López-Mesas, A. Heidlberger, K.P. Ishida, M. Reinhard, N-
452   nitrosodimethylamine (NDMA) removal by reverse osmosis and UV treatment and
453   analysis via LC-MS/MS, Water Res., 42 (2008) 347-355.

454   [11]   M.J. Farré, K. Döderer, L. Hearn, Y. Poussade, J. Keller, W. Gernjak, Understanding
455   the operational parameters affecting NDMA formation at Advanced Water Treatment
456   Plants, J. Hazard. Mater., 185 (2011) 1575-1581.

457   [12]   Y. Miyashita, S.-H. Park, H. Hyung, C.-H. Huang, J.-H. Kim, Removal of N-
458   Nitrosamines and their precursors by nanofiltration and reverse osmosis membranes, J.
459   Environ. Eng., 135 (2009) 788-795.

460   [13]   T. Fujioka, L.D. Nghiem, S.J. Khan, J.A. McDonald, Y. Poussade, J.E. Drewes,
461   Effects of feed solution characteristics on the rejection of N-nitrosamines by reverse
462   osmosis membranes, J. Membr. Sci., 409–410 (2012) 66-74.

463   [14]   P. Xu, C. Bellona, J.E. Drewes, Fouling of nanofiltration and reverse osmosis
464   membranes during municipal wastewater reclamation: Membrane autopsy results
465   from pilot-scale investigations, J. Membr. Sci., 353 (2010) 111-121.

466   [15]   R.Y. Ning, T.L. Troyer, Colloidal fouling of RO membranes following MF/UF in the
467   reclamation of municipal wastewater, Desalination, 208 (2007) 232-237.

468   [16]   L.D. Nghiem, S. Hawkes, Effects of membrane fouling on the nanofiltration of
469   pharmaceutically active compounds (PhACs): Mechanisms and role of membrane
470   pore size, Sep. Purif. Technol., 57 (2007) 176-184.

471   [17]   A.R.D. Verliefde, E.R. Cornelissen, S.G.J. Heijman, I. Petrinic, T. Luxbacher, G.L.
472   Amy, B. Van der Bruggen, J.C. van Dijk, Influence of membrane fouling by
473   (pretreated) surface water on rejection of pharmaceutically active compounds
474   (PhACs) by nanofiltration membranes, J. Membr. Sci., 330 (2009) 90-103.

475   [18]   K.O. Agenson, T. Urase, Change in membrane performance due to organic fouling in
476   nanofiltration (NF)/reverse osmosis (RO) applications, Sep. Purif. Technol., 55 (2007)
477   147-156.

478   [19]   K. Boussu, A. Belpaire, A. Volodin, C. Van Haesendonck, P. Van der Meeren, C.
479   Vandecasteele, B. Van der Bruggen, Influence of membrane and colloid
480   characteristics on fouling of nanofiltration membranes, J. Membr. Sci., 289 (2007)
481   220-230.

482   [20]   T. Fujioka, S.J. Khan, Y. Poussade, J.E. Drewes, L.D. Nghiem, N-nitrosamine
483   removal by reverse osmosis for indirect potable water reuse – A critical review based
484   on observations from laboratory, pilot and full scale studies, Manuscript submitted to
485   Separation and Purification Technology for publication, (2012).

486   [21]   R.K. Henderson, N. Subhi, A. Antony, S.J. Khan, K.R. Murphy, G.L. Leslie, V. Chen,
487   R.M. Stuetz, P. Le-Clech, Evaluation of effluent organic matter fouling in
488   ultrafiltration treatment using advanced organic characterisation techniques, J. Membr.
489   Sci., 382 (2011) 50-59.

490   [22]   S.A. Huber, A. Balz, M. Abert, W. Pronk, Characterisation of aquatic humic and non-
491   humic matter with size-exclusion chromatography – organic carbon detection –
492   organic nitrogen detection (LC-OCD-OND), Water Res., 45 (2011) 879-885.

493   [23]   J.A. McDonald, N.B. Harden, L.D. Nghiem, S.J. Khan, Analysis of N-nitrosamines in
494   water by isotope dilution gas chromatography-electron ionisation tandem mass
495   spectrometry, Talanta, (2012) Accepted 18 May 2012, doi:
496   2010.1016/j.talanta.2012.2005.2032.

497   [24]   J.E. Drewes, C. Bellona, M. Oedekoven, P. Xu, T.-U. Kim, G. Amy, Rejection of
498   wastewater-derived micropollutants in high-pressure membrane applications leading
499   to indirect potable reuse, Environ. Prog., 24 (2005) 400-409.

500   [25]   E. Van Houtte, J. Verbauwhede, Operational experience with indirect potable reuse at
501   the Flemish Coast, Desalination, 218 (2008) 198-207.

502   [26]   B. Spiegelhalder, R. Preussmann, Contamination of toiletries and cosmetic products
503   with volatile and nonvolatile N-nitroso carcinogens, J. Cancer Res. Clin. Oncol., 108
504   (1984) 160-163.

505   [27]   S.W. Krasner, P. Westerhoff, B. Chen, B.E. Rittmann, G. Amy, Occurrence of
506   disinfection byproducts in United States wastewater treatment plant effluents, Environ.
507   Sci. Technol., 43 (2009) 8320-8325.

508   [28]   R.K. Henderson, R.M. Stuetz, S.J. Khanz, Demonstrating ultra-filtration and reverse
509   osmosis performance using size exclusion chromatography, Water Sci. Technol., 62
510   (2010) 2747-2753.

511   [29]   J. Haberkamp, M. Ernst, U. Böckelmann, U. Szewzyk, M. Jekel, Complexity of
512   ultrafiltration membrane fouling caused by macromolecular dissolved organic
513   compounds in secondary effluents, Water Res., 42 (2008) 3153-3161.

17

514   [30]   H.K. Shon, S. Vigneswaran, R.B. Aim, H.H. Ngo, I.S. Kim, J. Cho, Influence of
515   Flocculation and Adsorption as Pretreatment on the Fouling of Ultrafiltration and
516   Nanofiltration Membranes: Application with Biologically Treated Sewage Effluent,
517   Environ. Sci. Technol., 39 (2005) 3864-3871.

518   [31]   L.D. Nghiem, P.J. Coleman, C. Espendiller, Mechanisms underlying the effects of
519   membrane fouling on the nanofiltration of trace organic contaminants, Desalination,
520   250 (2010) 682-687.

521   [32]   C.Y. Tang, Y.-N. Kwon, J.O. Leckie, Fouling of reverse osmosis and nanofiltration
522   membranes by humic acid--Effects of solution composition and hydrodynamic
523   conditions, J. Membr. Sci., 290 (2007) 86-94.

524   [33]   M. Beyer, B. Lohrengel, L.D. Nghiem, Membrane fouling and chemical cleaning in
525   water recycling applications, Desalination, 250 (2010) 977-981.

526   [34]   S. Lee, W.S. Ang, M. Elimelech, Fouling of reverse osmosis membranes by
527   hydrophilic organic matter: implications for water reuse, Desalination, 187 (2006)
528   313-321.

529   [35]   C.Y. Tang, Y.-N. Kwon, J.O. Leckie, Characterization of humic acid fouled reverse
530   osmosis and nanofiltration membranes by transmission electron microscopy and
531   streaming potential measurements, Environ. Sci. Technol., 41 (2006) 942-949.

532   [36]   V. Freger, Swelling and morphology of the skin layer of polyamide composite
533   membranes: an atomic force microscopy study, Environ. Sci. Technol., 38 (2004)
534   3168-3175.

535   [37]   Z. Chen, K. Ito, H. Yanagishita, N. Oshima, R. Suzuki, Y. Kobayashi, Correlation
536   study between free-volume holes and molecular separations of composite membranes
537   for reverse osmosis processes by means of variable-energy positron annihilation
538   techniques, The Journal of Physical Chemistry C, 115 (2011) 18055-18060.

539   [38]   K.L. Tu, A.R. Chivas, L.D. Nghiem, Effects of membrane fouling and scaling on
540   boron rejection by nanofiltration and reverse osmosis membranes, Desalination, 279
541   (2011) 269-277.

542   [39]   H.Y. Ng, M. Elimelech, Influence of colloidal fouling on rejection of trace organic
543   contaminants by reverse osmosis, J. Membr. Sci., 244 (2004) 215-226.

544   [40]   C. Bellona, J.E. Drewes, P. Xu, G. Amy, Factors affecting the rejection of organic
545   solutes during NF/RO treatment - A literature review, Water Res., 38 (2004) 2795-
546   2809.

547

548 **Table 1**: Properties of the membranes used in this study.

Membrane	Pure water permeability[a] [L/m^{2}hbar]	Conductivity rejection[b] [%]
NF90	11.7 ± 1.1	81.2 ± 2.5
ESPA2	5.5 ± 0.3	98.1 ± 0.3
ESPAB	3.9 ± 0.2	99.3 ± 0.4

549 [a] Determined with Milli-Q water at 1,000 kPa and 20 °C feed temperature. Errors represent

550 the standard deviation of three replicates.

551 [b] Analysed with feed solution contained 20 mM NaCl, 1 mM NaHCO$_3$, 1 mM CaCl$_2$ at

552 permeate flux 20 L/m^{2}h, cross flow velocity 40.2 cm/s, feed pH 8.0 ± 0.1 and feed

553 temperature 20.0 ± 0.1 °C.

554 **Table 2:** Water quality of the tertiary effluent.

Parameter	Value
Turbidity	0.7 NTU
Conductivity	790 µS/cm
pH	7.8
TOC	9.3 mg/L
Na^+	106 mg/L
Mg^{2+}	14 mg/L
K^+	17 mg/L
Ca^{2+}	23 mg/L
Fe^{2+}	13 mg/L
Cl^-	177 mg/L
NO_3^-	43 mg/L
SO_4^{2-}	46 mg/L

555

556 **Table 3:** Organic matter fractions in each feed solution.

	Tertiary effluent	BSA	Sodium alginate	Humic acid
Hydrophobic [%]	11.1	n.q.	2.0	0.4
Hydrophilic				
Biopolymer [%]	9.8	79.5	91.1	5.6
Humics [%]	50.8	n.q.	n.q.	68.4
(Mean MW [g/mol])	(467)			(850)
Building blocks [%]	15.1	8.1	2.2	9.2
LMW neutrals [%]	12.6	22.4	2.6	16.4
LMW acid [%]	0.6	0.2	2.1	n.q.

557 *n.q., not quantifiable

Effects of membrane fouling on N-nitrosamine rejection by nanofiltration and reverse osmosis membranes

Journal of Membrane Science

Takahiro Fujioka [1], Stuart J. Khan [2], James A. McDonald [2], Rita K. Henderson [2], Yvan Poussade [3,4], Jörg E. Drewes [2, 5], and Long D. Nghiem [1,*]

[1] Strategic Water Infrastructure Laboratory, School of Civil Mining and Environmental Engineering, The University of Wollongong, NSW 2522, Australia

[2] UNSW Water Research Centre, School of Civil and Environmental Engineering, The University of New South Wales, NSW 2052, Australia

[3] Veolia Water Australia, Level 15, 127 Creek Street, QLD 4000, Australia

[4] Seqwater, Level 2, 240 Margaret St, Brisbane City QLD 4000 Australia

[5] Advanced Water Technology Center (AQWATEC), Department of Civil and Environmental Engineering, Colorado School of Mines, Golden, CO 80401, USA

SUPPLEMENTARY MATERIAL

_____

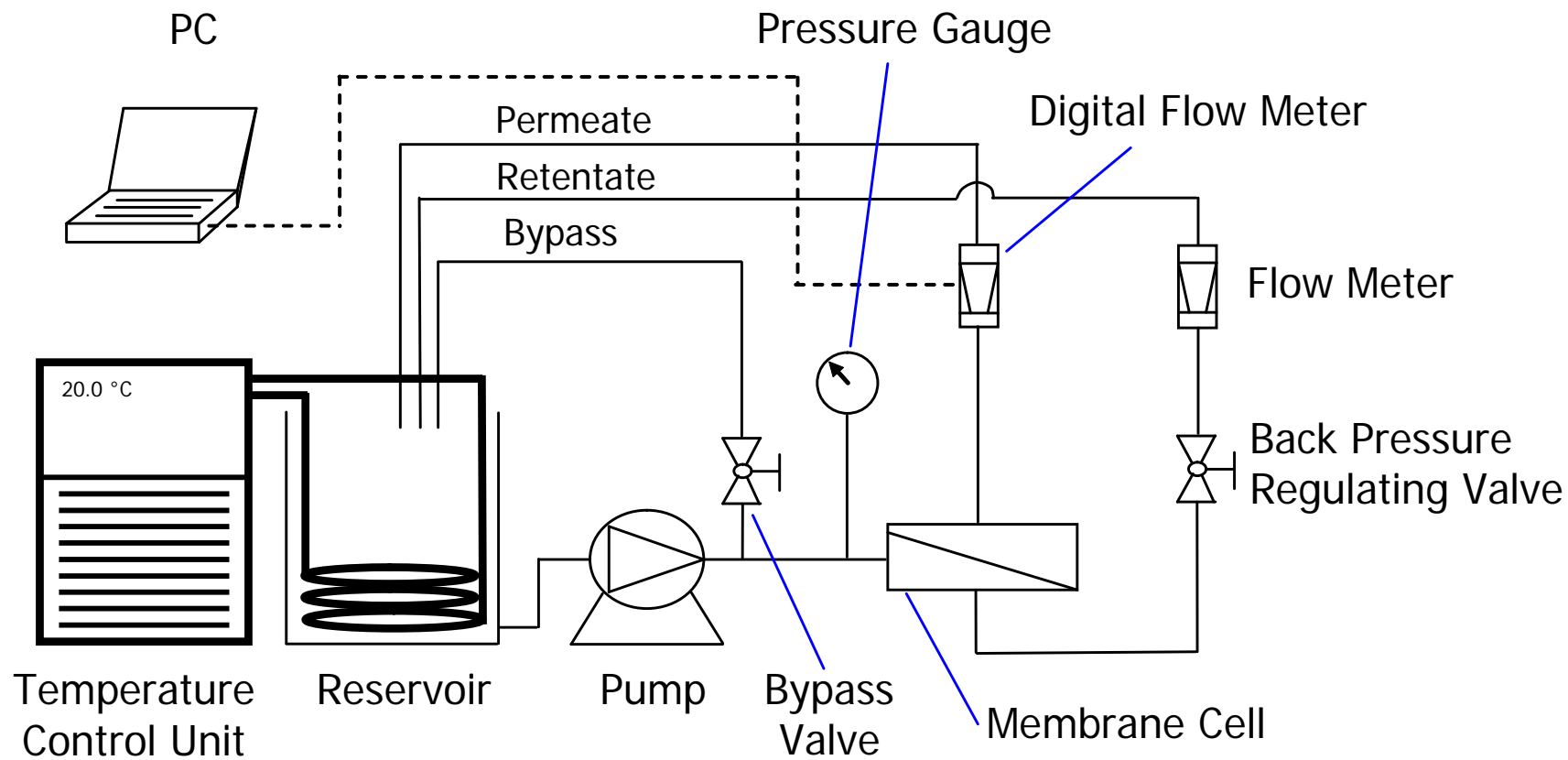* Corresponding author: Long Duc Nghiem, Email: longn@uow.edu.au, Ph +61 2 4221 4590

Figure S1: Schematic diagram of the cross flow filtration system.

Table S2: Membrane permeability by the clean and fouled membranes.

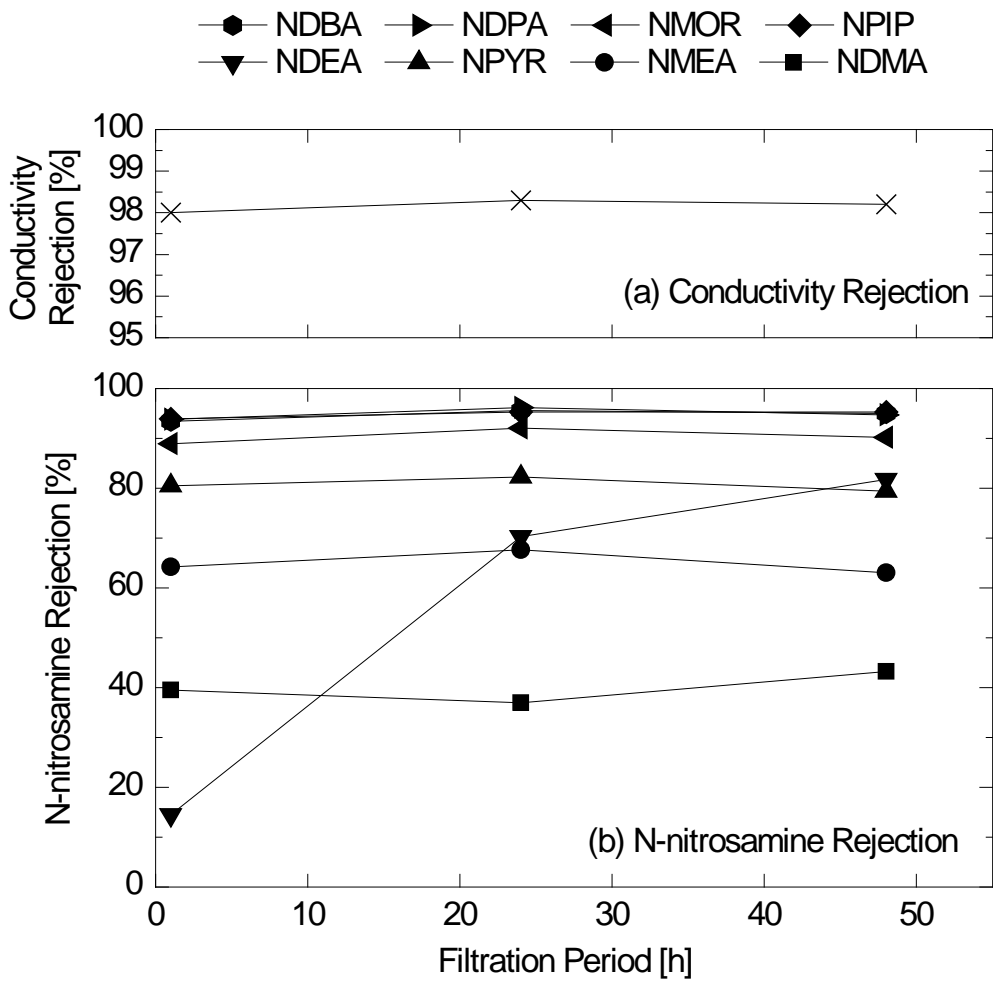| Membrane	Feed solution		Clean [Lm^{-2}h^{-1}bar^{-1} at 20°C]	Fouled [Lm^{-2}h^{-1}bar^{-1} at 20°C]
NF90	Tertiary effluent		11.1	5.7
ESPAB	Tertiary effluent		3.3	2.7
ESPA2	Tertiary effluent	1st	4.9	3.6
		2nd	5.0	3.5
	Sodium alginate	1st	4.5	2.6
		2nd	4.6	3.0
	Humic acid	1st	5.0	2.9
		2nd	5.0	3.6
	BSA	1st	4.7	4.0
		2nd	4.7	3.7
	Ludox CL	1st	4.9	3.5
		2nd	4.7	3.3

Figure S3: (a) Conductivity rejection and (b) N-nitrosamine rejection by the ESPA2 membrane as a function of filtration period (permeate flux 20 L/m^{2}h, crossflow velocity 40.2 cm/s, feed temperature 20.0 ± 0.1 °C).
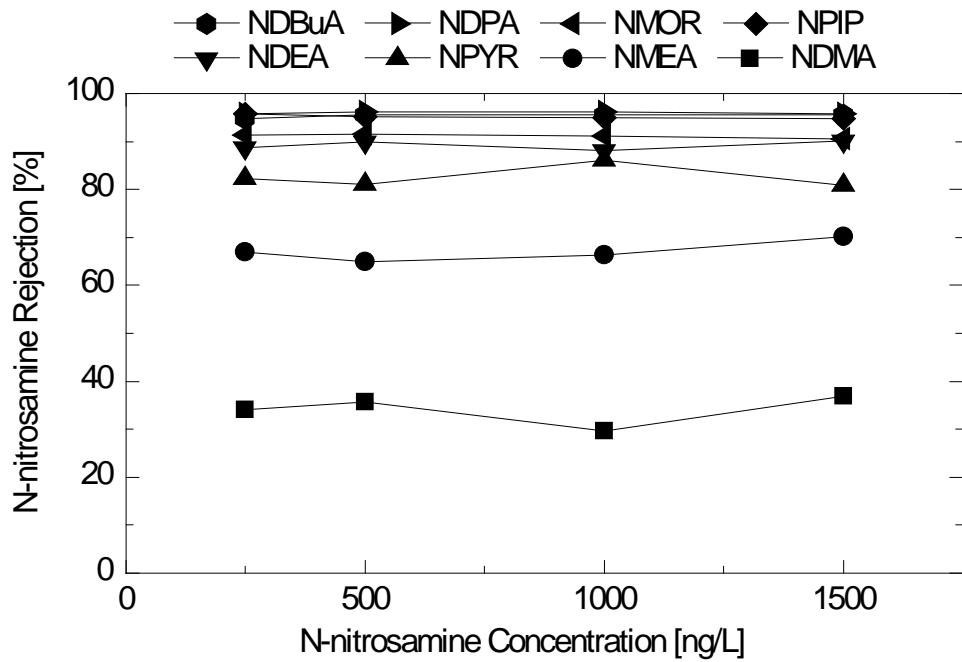
Figure S4: Rejection of N-nitrosamines by ESPA2 membrane as a function of nitrosamine concentration in the feed (20 mM NaCl, 1 mM NaHCO$_3$, 1 mM CaCl$_2$, permeate flux 20 L/m^{2}h, crossflow velocity 40.2 cm/s, feed pH 8.0$\pm$0.1, feed temperature 20.0$\pm$0.1 °C).